AGU PUBLICATIONS

Geophysical Research Letters

RESEARCH LETTER

10.1002/2016GL069151

Key Points:
- Historical CMIP5 simulations shift the EPI from summer to spring for most regions
- A future increase in seasonal contribution of the EPI during winter is projected for most regions
- The summer to spring shift in the EPI is projected to increase for most regions through 2100

Supporting Information:
- Supporting Information S1

Correspondence to:
E. Janssen,
ejansse2@illinois.edu

Citation:
Janssen, E., R. L. Sriver, D. J. Wuebbles, and K. E. Kunkel (2016), Seasonal and regional variations in extreme precipitation event frequency using CMIP5, *Geophys. Res. Lett.*, *43*, 5385–5393, doi:10.1002/2016GL069151.

Received 22 JAN 2016
Accepted 13 MAY 2016
Accepted article online 16 MAY 2016
Published online 31 MAY 2016

Seasonal and regional variations in extreme precipitation event frequency using CMIP5

E. Janssen[1], R. L. Sriver[1], D. J. Wuebbles[1], and K. E. Kunkel[2]

[1]Department of Atmospheric Sciences, University of Illinois, Urbana, Illinois, USA, [2]Cooperative Institute for Climate and Satellites-NC, North Carolina State University and NOAA National Centers for Environmental Information, Asheville, North Carolina, USA

Abstract Understanding how the frequency and intensity of extreme precipitation events are changing is important for regional risk assessments and adaptation planning. Here we use observational data and an ensemble of climate change model experiments (from the Coupled Model Intercomparison Project Phase 5 (CMIP5)) to examine past and potential future seasonal changes in extreme precipitation event frequency over the United States. Using the extreme precipitation index as a metric for extreme precipitation change, we find key differences between models and observations. In particular, the CMIP5 models tend to overestimate the number of spring events and underestimate the number of summer events. This seasonal shift in the models is amplified in projections. These results provide a basis for evaluating climate model skill in simulating observed seasonality and changes in regional extreme precipitation. Additionally, we highlight key sources of variability and uncertainty that can potentially inform regional impact analyses and adaptation planning.

1. Introduction

Numerous studies show statistically significant increases in frequency and intensity of extreme precipitation over much of the United States [*Karl et al.*, 1996; *Karl and Knight*, 1998; *Groisman et al.*, 2004, 2005, 2012; *Kunkel et al.*, 1999, 2003, 2007, 2012b; *Karl et al.*, 2009; *Alexander et al.*, 2006; *Min et al.*, 2011; *Janssen et al.*, 2014] and the rest of the world [*Lehmann et al.*, 2015; *Donat et al.*, 2016]. Climate model projections point to continued future increases in extreme precipitation events over the United States, including areas where mean precipitation is expected to decrease [*Wehner*, 2012; *Kunkel et al.*, 2012b; *Wuebbles et al.*, 2013; *Janssen et al.*, 2014]. The physical cause of these increases in extreme precipitation is due to increases in saturation vapor pressure. The maximum amount of water in vapor form is governed by the Clausius-Clapeyron equation which calls for a 7% change per degree Kelvin of temperature change [*Trenberth et al.*, 2003]. Atmospheric water content should increase accordingly, allowing for heavier precipitation events. However, the rate of precipitation increase over land is not expected to be as large as increases over the oceans [*Allen and Ingram*, 2002; *Wentz and Schabel*, 2000; *Trenberth et al.*, 2003; *Pall et al.*, 2007; *Santer et al.*, 2007; *Willett et al.*, 2007; *Min et al.*, 2011].

The extreme precipitation index (EPI) [*Kunkel et al.*, 1999, 2003, 2007; *Janssen et al.*, 2014] is an empirical indicator which measures the frequency of extreme precipitation events for a given duration and expected return interval. The EPI shows an annual increase over many regions of the United States historically (1901–2012) and for projections (2006–2100) using the Representative Concentration Pathway (RCP) 4.5 and 8.5 scenarios. Observational trends are captured by simulations from phase 5 of the Coupled Model Intercomparison Project (CMIP5); however, the simulated magnitude of events in the CMIP5 models tends to be smaller than observed [*Janssen et al.*, 2014]. *Kunkel et al.* [2012a, 2012b] provide a historical analysis of the meteorology associated with observed station extreme events (1908–2009). They isolate distinct meteorological phenomena over the United States and the (temporal or spatial) trends associated with observed events. It is found that the frequency of events near frontal boundaries associated with extratropical cyclones are increasing; they did not determine whether this was due to overall changes in frontal climatology or changes in the efficiency of extreme event production from fronts.

Wehner [2012] analyzes simulations of seasonal daily extreme precipitation over the contiguous United States (CONUS) through a comparison of eight North American Regional Climate Change Assessment Program (NARCCAP) models to two gridded observational data sets. Using several metrics measuring model performance, the study shows that NARCCAP models vary significantly in their ability to simulate observed precipitation extremes. While this study has advantages in that it uses higher resolution regional models, it is limited by the relatively low number of models and ensembles used compared to that of the suite of models from the fifth installment of the Coupled Model Intercomparison Project (CMIP5). *Wehner* [2012] shows projections with statistically significant increases in mean precipitation for the upper United States during winter and decreases in the west during summer and southwest in the spring. However, correlations between seasonal mean and extreme precipitation decreases with rarity of events, thus the same skill found for mean precipitation cannot be carried over to extremes.

While the aforementioned studies investigate aspects of extreme precipitation, there remains a need for a comprehensive understanding of the ability of global climate model (GCM) simulations, using a larger number of ensembles, to capture observed seasonality of extreme precipitation. Here we build on previous research efforts analyzing extreme precipitation by addressing three key questions: (1) Do CMIP5 models capture observed seasonality of extreme precipitation? (2) Do CMIP models capture observed trends in seasonal extreme precipitation event frequency? (3) What do the CMIP5 GCMs project for future seasonal extreme precipitation frequency? This study provides a regional analysis of observed trends and seasonality of extreme precipitation frequency over the United States from 1901 to 2014 using the EPI. We assess the ability of GCMs to simulate the seasonality of the EPI using the entire suite of CMIP5 models. Additionally we explore the ability of CMIP5 models to capture observed natural variability of the EPI. Trends in projections of seasonal extreme precipitation event frequency over the contiguous United States (CONUS) are also investigated using the RCP 8.5 for the suite of CMIP5 models.

2. Data

Observed daily precipitation data are from the U.S. Cooperative Observer Network, as included in the Global Historical Climate Network-Daily data set from the National Climatic Data Center. The data are updated from *Janssen et al*. [2014] and now run from 1901 to 2014 with an additional 40 stations for a total of 766 stations over CONUS. When used for comparison with historical CMIP5 model simulations, the observational time period used is 1901–2005 due to model simulations ending in 2005. The data are quality control tested and corrected by *Kunkel et al*. [2005]; they identified one major issue which is a shift from predominantly afternoon observations in the early part of the record to mainly morning observations in the more recent record but this is not known to cause biases in the extremes of precipitation. Precipitation data used in this study are composed of liquid or liquid water equivalent precipitation. While prior studies show that about 2% of extreme precipitation events are considered either partial or complete snowfall [*Kunkel et al*., 2012a, 2012b], we do not differentiate between snow and rain events in this analysis.

We use a total of 27 different models for the hindcast analysis and 21 different models for the projections [*Taylor et al*., 2009, 2012]. One drawback in using CMIP5 model output is the mismatch between the historical modeled hindcast record (1901–2005) and the observations time range (1901–2014). Projections are forced by the RCP 8.5 scenario for the time range of 2006–2100. Each RCP scenario makes different assumptions for greenhouse gas concentrations and other factors which affect the Earth's climate system. Extensive details on the RCPs can be found in *Moss et al*. [2010] and *Van Vuuren et al*. [2011]. Here we utilize RCP 8.5 which serves as high and emission scenario.

We present intermodel comparisons in which we analyze a combination of single simulations from each different model (totaling 27 simulations for hindcasts and 21 for projections) as well as all available ensemble members for all models (totaling 94 simulations for hindcasts and 51 simulations for projections). The models used in this analysis are referenced in the supporting information.

3. Methodology

The EPI utilizes station specific thresholds rather than predetermined threshold amounts which results in equal weighting of stations regardless of their extreme precipitation climatology. We examine events of a 2 day duration exceeding a station-specific threshold for a 5 year return interval. Larger return intervals show similar results annually [*Janssen et al*., 2014]. A station is considered usable when at least 90% of the daily data is available in a time series. Any given year in a station time series is used only if at least 300 days of data are available [*Janssen et al*., 2014]. All 766 stations are available after this process. It should be noted that with a 1° grid spacing, and only 766 reporting stations, some grid cells will have zero reporting stations. This

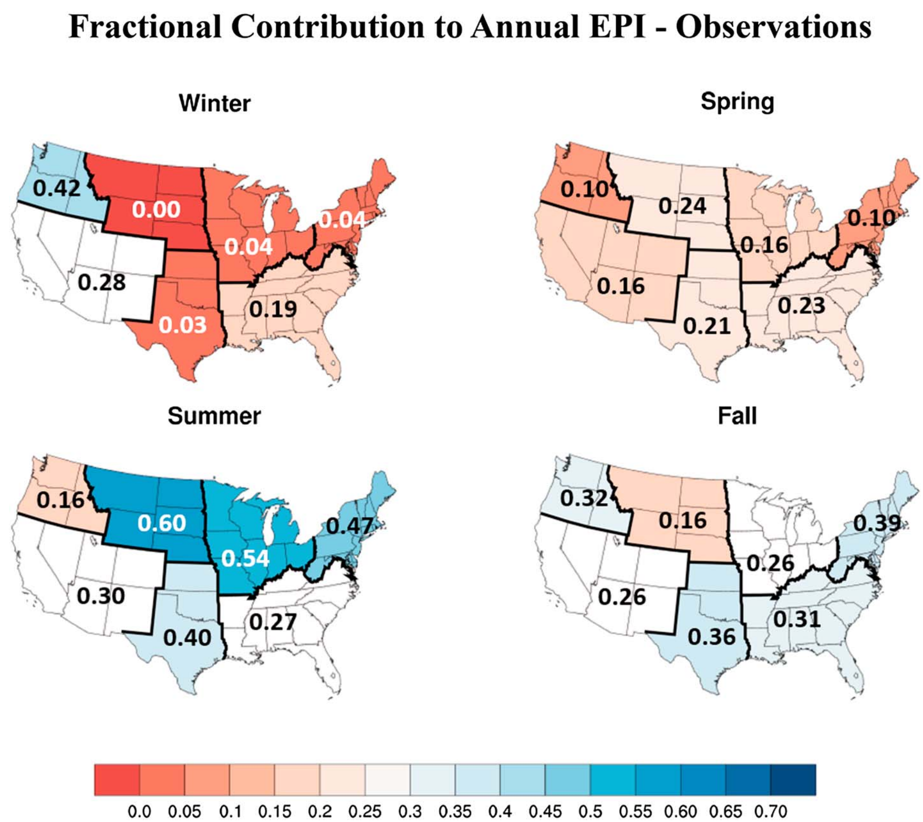

Figure 1. Observation-based, fractional contribution of average seasonal EPI to the average annual EPI for the time period of 1901–2005. Numbers are the average fractional contribution and correspond to color of respective regions.

occurs most frequently in the western U.S. For the seasonal analysis, every season is required to have at least 75 days of usable data. It is unusual for these criteria to not be met. For example, when considering the CONUS, from 1901 to 2005, events that meet the criteria for winter spring and fall all equal or round to 100%. For summer, 97.2% of the events meet the criteria. If these conditions are not met, the year, season, and/or station are ignored in the analysis. Seasons are defined as follows: winter (December-January-February), spring (March-April-May), summer (June-July-August), and fall (September-October-November). For any given winter, the December from the previous year is used. For regional and national analyses, station event time series are averaged for 1° latitude × 1° longitude grid cells.

Stations are initially split into regions via state identifiers. The number of events per station is found as follows: First the number of events (N) is calculated by taking the length of the time series in years and dividing by the average return period (i.e., 5 years). For any given station, the largest magnitude event in the time series is counted or “flagged” and both year and season of occurrence are recorded. The event is ranked as the largest, and those days are subsequently removed from the time series. Then, the next largest event is flagged, year and season recorded, and again removed. This continues in an iterative fashion until N events have been flagged, counted, and removed from the time series. Annual and seasonal time series of the frequency of extreme precipitation events are constructed as counts of these N events by year. These counts, split up by season, are averaged over all the stations contained in each grid cell giving the average time series for each grid cell for each season. The grid cells are then averaged over each region and the entire CONUS for every season. This process gives the frequency of extreme precipitation events for each season (EPI), and adding each season gives the annual frequency of events. Statistical significance (usually to the 95% confidence level) is tested by taking a linear regression fit to a Poisson’s distribution for a given time series for each region.

For CMIP5 model simulations, the seasonal 2 day 5 year EPI is calculated in the same manner as observations. We apply four different ensemble averaging approaches in order to assess the robustness of the results. In the main text, we highlight the results using multimodel ensemble means that include all available

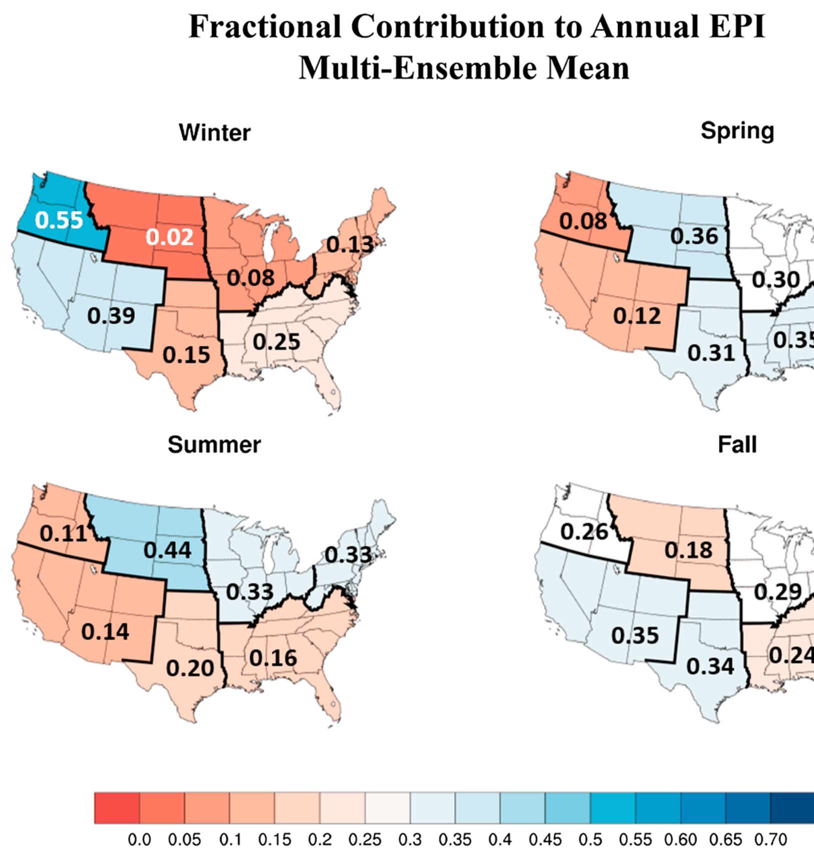

Figure 2. The model mean fractional contribution of average seasonal EPI to the average annual EPI for CMIP5 simulations. Numbers are the average fractional contribution and correspond to color of respective regions.

simulations. In the supporting information, we include additional results based on the multimodel ensemble mean using a single simulation from all available models. We also repeat these analyses using the ensemble median based on both single-member and multimember ensemble approaches described above (see supporting information for more details). Because CMIP5 simulations end in 2005, observation-based EPI is recalculated for 1901–2005 to compare model simulations.

RCP-forced CMIP5 projections are analyzed for each season using RCP 8.5. This index follows a slightly different procedure than the historical EPI calculation. The top *N* events from 2006 to 2100 are found for a 2 day 5 year return based on thresholds determined using the historical simulations. For each historical model EPI time series, the smallest *N*th event found for each grid cell is set as the threshold amount for the corresponding model and ensemble. Then the top *N* events that fall above that threshold for each time series are found in the same iterative manner used previously for each ensemble. The season and year of occurrence are recorded to find the seasonal EPI for projections. The regional EPI is calculated for each simulation by averaging over grid cells. The ensemble mean is then found across all simulations. For the supporting information, the methods match those of the historical simulations.

The ratio of the seasonal to annual EPI is used to examine seasonality for each region and the CONUS for historical models, observations, and projections. For observations, the EPI was recalculated for the time period of 1901–2005 in order to compare to models. Two methods comparing models to observations are used. The first method involves averaging over each regional time series of the EPI for each season and the annual. Then we calculate the fractional contribution to the annual for models and observations. This process is repeated using the other three techniques outlined (see supporting information). The second method consists of finding correlation coefficients between model median time series and observational time series. First, the fractional contribution of seasonal to annual, for each year, is calculated for the entire time series of 1901–2005. Then correlation coefficients are calculated, comparing observations to model mean fractions. Through the use of these two methods we assess the ability of CMIP5 simulations to capture observed seasonality in the EPI.

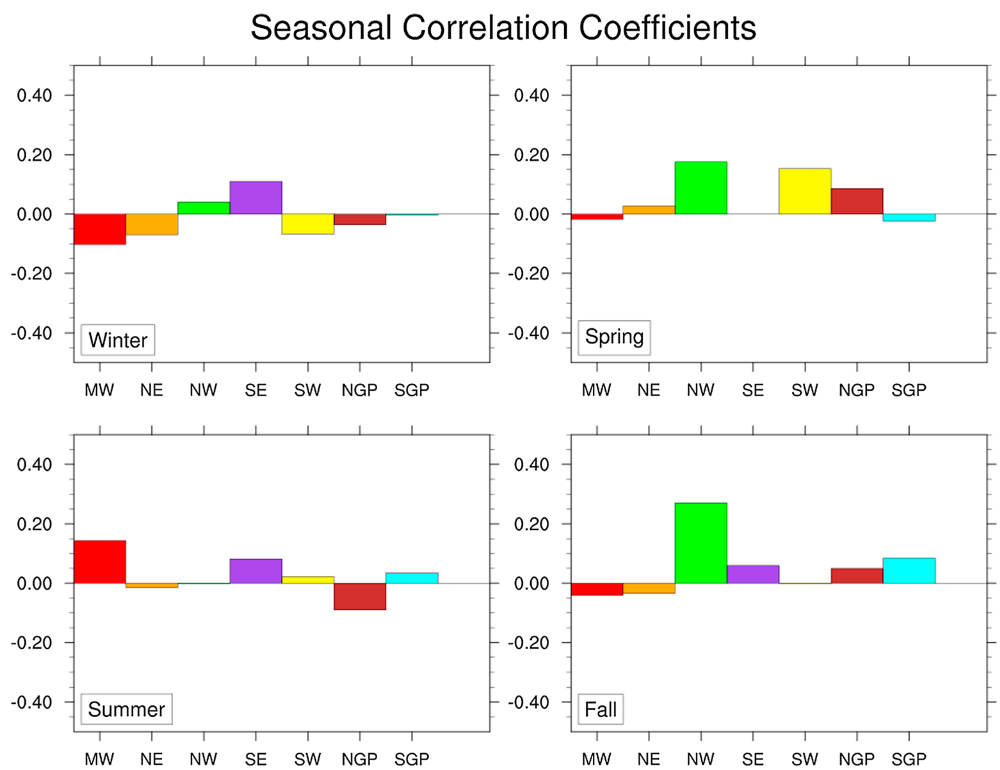

Figure 3. Correlation coefficients comparing the fractional contribution of seasonal to annual EPI. The time series (1901–2005) are used for observational and model-based EPI.

4. Results and Discussion

Examining overall seasonal contribution to the annual, Figure 1 shows the average fractional EPI contribution to the annual for each season regionally. Summer provides the highest contribution to annual EPI for the central and northeastern regions of the United States. During the fall, we see moderate contributions in all regions. Winter is the smallest for all regions aside from the west with a maximum contribution in the northwest over all seasons.

We analyze seasonal extreme precipitation event frequency trends using the EPI from 1901 to 2014 (see supporting information). We find that midwestern summer dominates the contribution to the annual for the EPI with a slight increasing trend overall. During the fall, there is a recent increase in contribution to annual in the eastern United States, especially the southeast. Winter provides a large contribution in the west, particularly the northwest. This is expected, as the western United States receives the bulk of their precipitation during the winter [*Higgins et al*., 2000 and *Kunkel et al*., 2012a, 2012b]. We find that none of the seasonal trends are statistically significant for any region using a Poisson's distribution significance test. However, when examined by grid point, many locations show statistically significant trends to the 95th percent confidence interval for seasonal EPI, tested by taking a linear regression fit to a Poisson's distribution.

Seasonal EPI simulations show a smaller magnitude compared to observations, while still capturing any observed trends, similar to the annual result of *Janssen et al*. [2014]. However, some regions show no observed or simulated seasonal trends at all. Figure 2 shows the fractional contribution of seasonal EPI to the annual for the mean of CMIP5 models. We see general agreement with observations during the winter, although models increase events in most regions. *Sheffield et al*. [2013] show that during winter, several of the higher-resolution CMIP5 models produce divergence that is too strong along the U.S. coasts and precipitation is overestimated by these models. Thus, this overestimation could be due to model differences in the underlying large-scale dynamics.

The largest difference between models and observations is the reduction of events in the models during the summer months for every region of the CONUS. The models subsequently increase events in the spring for all

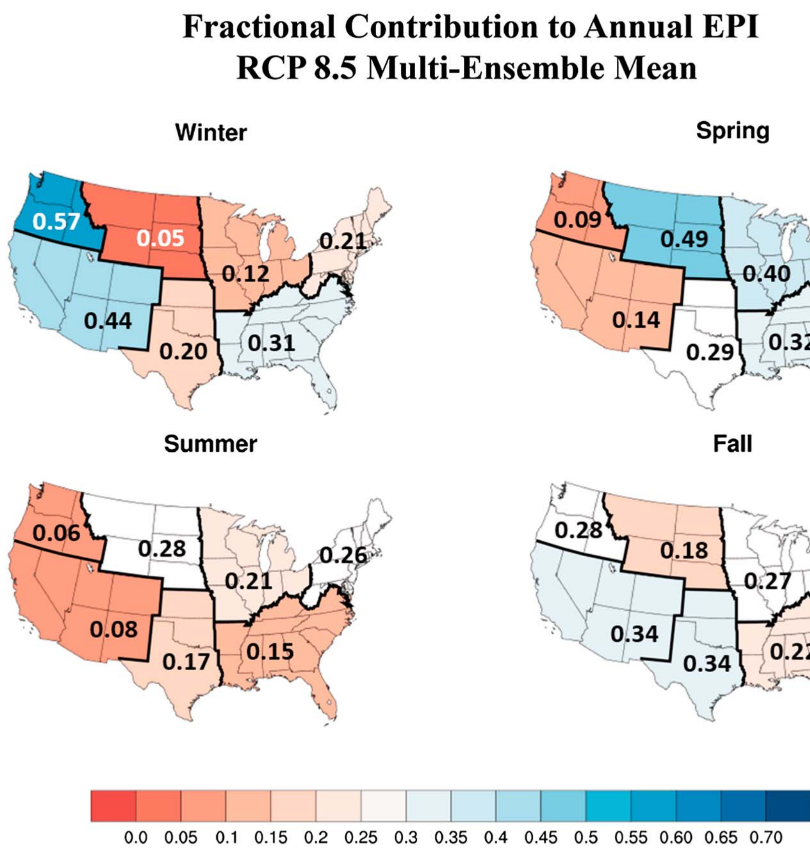

Figure 4. Model mean projections of the fractional contribution of average seasonal EPI to the average annual EPI using the RCP 8.5 scenario. Numbers are the fractional contribution and correspond to color of respective regions.

regions, except the west, indicating that the models are simulating more extreme precipitation events earlier in the warm season. There are several possible reasons for this shift in the models. Global models used in CMIP5 do not typically resolve orographic features such as mountain ranges, which for the central United States are an important contribution to the environmental conditions which produce extreme precipitation events. *Sheffield et al*. [2013] find that even for five higher-resolution CMIP5 models, the strong convergence over the Rockies and Mexican Plateau is not well captured and is associated with a low bias in mean precipitation found for those regions. Other contributing factors could be the ability of the models to simulate convection and mesoscale processes associated with tropical cyclones and fronts. In the latter case, *Kunkel et al*. [2012a, 2012b] found that fronts were an important cause of summer heavy events, even in the southeast U.S. While we are not aware of studies examining summer fronts, these features may not be simulated adequately by global models because the gradients and associated low-level convergence are generally quite weak in the summer, although adequate to trigger convection in the conditionally unstable atmosphere typical of summer in the eastern U.S. Models tend to agree with observations in the fall with small differences between regions, the largest being an increase in models in the southwest.

Figure 3 shows correlation coefficients comparing the fractional contribution time series between the multimodel ensemble mean (94 total simulations from 27 different models) and observations for each region and season. The northwestern region shows the best agreement with observations, particularly in the spring and fall. The models are particularly well correlated to observations during the spring for the western United States. This largely matches what we see in the fractional contribution maps and the EPI time series. During summer, the midwest shows positive correlation between the models and observations; however, the average model contribution for summer in the midwest shows an underestimation by about 16%. This suggests that the models capture time series trends while failing to capture the average contribution to the annual for this region during the summer. This is a common occurrence for several regions during various seasons.

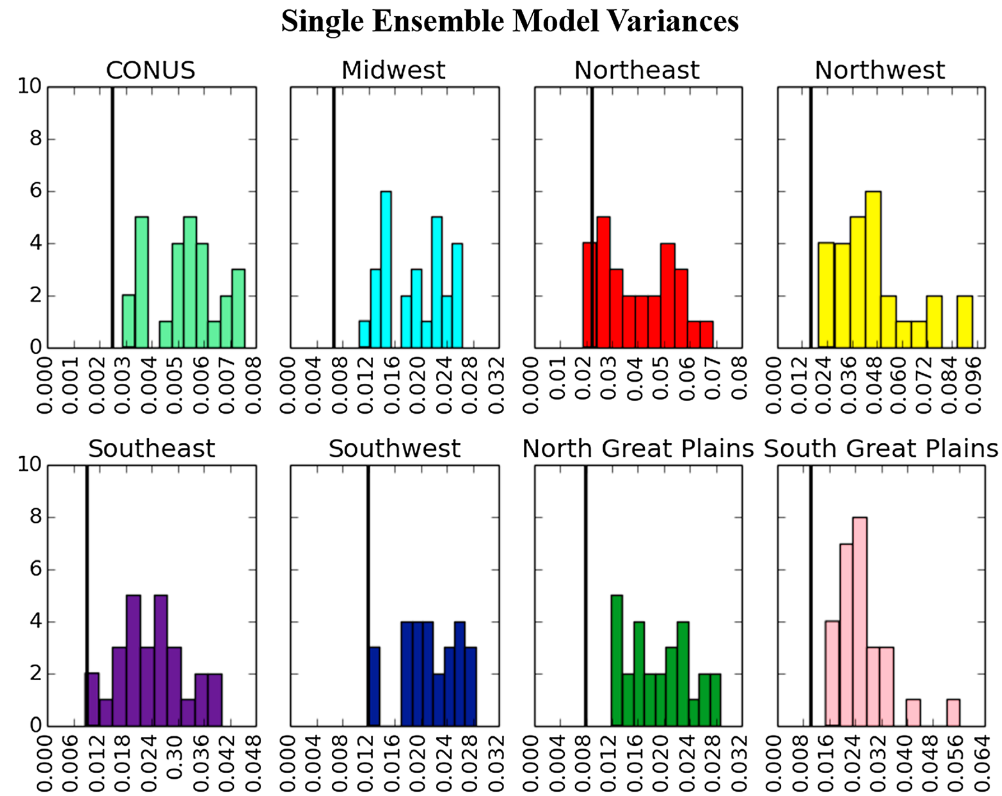

Figure 5. EPI variances for each CMIP5 model plotted as histograms. We calculate variance using a single historical simulation (1901–2005) from each different model. The bold black line represents observation-based EPI variance.

Projections of average seasonal contributions to annual for the EPI (2006–2100) are shown in Figure 4. The winter contribution increases for all regions compared to both historical models and observations. Projected changes during the fall are relatively small over all regions of the United States. There is a distinct shift of events from summer to spring in projections when compared to observations. Projections show decreases in all regions during summer and subsequent increases in spring for all but the western regions. Summer contributions decrease at least slightly for all regions when compared to historical model means. There are increases in the spring when compared to historical models for the North Great Plains, midwest and northeast regions, and very small increases in the west, but the CMIP5 historical simulations place more events in spring and less in summer compared to observations. Thus, it is important to consider that these projected decreases in summer and increases in spring could be a product of the models and not due to the underlying physics. Because of the historical shift in the models, projections could be amplifying any real shift from summer to spring, causing an overproduction of events in spring and an underproduction in summer. This result may provide important constraints for regional impact analyses (e.g., agriculture) that use seasonal climate information from CMIP5 style models.

Internal variability represents the year-to-year "natural" variations in observed and modeled climate variables within the Earth's system [*Hawkins and Sutton*, 2009; *Flato et al.*, 2013; *Collins et al.*, 2013; *Sriver et al.*, 2015], which is largely filtered out when averaging over multiple times series. Here we extend our CMIP ensemble analysis to characterize the representation of internal variability of EPI within different models. Figure 5 shows histogram plots of model variances of the annual EPI for each region using a single simulation for each model. We find that most models tend to produce natural variability that is larger than observations for all regions. Large variances in the modeled annual EPI indicate that models cluster extreme precipitation events together while observations are smoother in time. A potential cause for this result is the underrepresentation of precipitation intensity in climate models compared to observations [*Sriver et al.*, 2015]. These results suggests that individually the models do a poor job capturing observed natural variability and that structural model differences and natural variability can both potentially influence interpretations about projected seasonal changes in extreme precipitation.

5. Conclusions

Observational EPI shows that seasonal contribution to annual is maximized in the summer for most regions. Historically, winter is at a minimum for most regions with the exception of the western United States. Historical CMIP5 simulations of seasonal contributions to the annual EPI show a shift of events from summer to spring for most regions when compared to observations. During the winter, the models capture the small contribution for most regions and the larger contributions for the western regions, including the southeast with a slight overproduction in most regions.

A future increase in seasonal contribution of the EPI during winter is projected for most regions. There is a shift in event frequency from summer to spring for most regions when compared to historical model and observation-based EPI. It is difficult to interpret the physical relevance of this projected seasonal shift given the seasonal differences in EPI between models and observations for the historical period. When considering single simulations from each model, we find that most models tend to overestimate internal variability in EPI compared to observations. Overall the CMIP5 ensemble as a whole generally captures seasonal contributions to annual EPI, with several key apparent model-data discrepancies. Results point to EPI as a useful diagnostic for examining extreme precipitation in Earth system models, which can have important implications for analyzing and interpreting projected changes in seasonal extreme precipitation event frequency.

Acknowledgments
This work was partially supported by NOAA through the Cooperative Institute for Climate and Satellites-North Carolina under cooperative agreement NA14NES432003. Observational daily precipitation data used in this study can be accessed via https://www.ncdc.noaa.gov/oa/climate/ghcn-daily/. We acknowledge the World Climate Research Programme's Working Group on Coupled Modeling, which is responsible for CMIP, and we thank the climate modeling groups (listed in Table 1 in the supporting information) for producing and making available their model output. For CMIP, the U.S. Department of Energy's Program for Climate Model Diagnosis and Intercomparison provides coordinating support and led development of software infrastructure in partnership with the Global Organization for Earth System Science Portals. CMIP5 data can be accessed via http://cmip-pcmdi.llnl.gov/cmip5/data_getting_started.html.

References

Alexander, L. V., et al. (2006), Global observed changes in daily climate extremes of temperature and precipitation, *J. Geophys. Res.*, *111*, D05109, doi:10.1029/2005JD006290.

Allen, M. R., and W. J. Ingram (2002), Constraints on future changes in climate and the hydrologic cycle, *Nature*, *419*, 224–232.

Collins, M., et al. (2013), Long-term climate change: Projections, commitments and irreversibility, in *Climate Change 2013: The Physical Science Basis. Contribution of Working Group I to the Fifth Assessment Report of the Intergovernmental Panel on Climate Change*, edited by T. F. Stocker et al., pp. 1029–1136, Cambridge Univ. Press, Cambridge, U. K., and New York, doi:10.1017/CBO9781107415324.024.

Donat, M. G., A. L. Lowry, L. V. Alexander, P. A. O'Gorman, and N. Maher (2016), More extreme precipitation in the world's dry and wet regions, *Nat. Clim. Change*, doi:10.1038/nclimate2941.

Flato, G., et al. (2013), Evaluation of climate models, in *Climate Change 2013: The Physical Science Basis. Contribution of Working Group I to the Fifth Assessment Report of the Intergovernmental Panel on Climate Change*, edited by T. F. Stocker et al., pp. 741–882, Cambridge Univ. Press, Cambridge, U. K., and New York, doi:10.1017/CBO9781107415324.020.

Groisman, P. Y., R. W. Knight, T. R. Karl, D. R. Easterling, B. Sun, and J. H. Lawrimore (2004), Contemporary changes of the hydrological cycle over the contiguous United States: Trends derived from in situ observations, *J. Hydrometeorol.*, *5*, 64–85.

Groisman, P. Y., D. R. Easterling, T. R. Karl, G. C. Hegerl, and V. N. Razuvaev (2005), Trends in intense precipitation in the climate record, *J. Clim.*, *18*, 1326–1350.

Groisman, P. Y., R. W. Knight, and T. R. Karl (2012), Changes in intense precipitation over the central United States, *J. Hydrometeorol.*, *13*, 47–66, doi:10.1175/JHM-D-11-039.1.

Hawkins, E., and R. Sutton (2009), The potential to narrow uncertainty in regional climate predictions, *Bull. Am. Meteorol. Soc.*, *90*, 1095–1107.

Higgins, R. W., J.-K. E. Schemm, W. Shi, and A. Leetmaa (2000), Extreme precipitation events in the western United States related to tropical forcing, *J. Clim.*, *13*, 793–820, doi:10.1175/1520-0442(2000)013<0793:EPEITW>2.0.CO;2.

Janssen, E., D. J. Wuebbles, K. E. Kunkel, S. C. Olsen, and A. Goodman (2014), Trends and projections of extreme precipitation over the contiguous United States, *Earth's Future*, *2*(2), 99–113, doi:10.1002/2013EF000185.

Karl, T. R., and R. W. Knight (1998), Secular trends of precipitation amount, frequency, and intensity in the United States, *Bull. Am. Meteorol. Soc.*, *79*, 231–241.

Karl, T. R., R. W. Knight, D. R. Easterling, and R. G. Quayle (1996), Indices of climate change for the United States, *Bull. Am. Meteorol. Soc.*, *77*, 279–292, doi:10.1175/1520-0477(1996)077<0279:IOCCFT>2.0.CO;2.

Karl, T. R., J. M. Melillo, and T. C. Peterson (Eds.) (2009), *Global Climate Change Impacts in the United States*, pp. 189, Cambridge Univ. Press, New York.

Kunkel, K. E., K. Andsager, and D. R. Easterling (1999), Long-term trends in extreme precipitation events over the conterminous United States and Canada, *J. Clim.*, *12*, 2515–2527.

Kunkel, K. E., D. R. Easterling, K. Redmond, and K. Hubbard (2003), Temporal variations of extreme precipitation events in the United States: 1895–2000, *Geophys. Res. Lett.*, *30*(17), 1900, doi:10.1029/2003GL018052

Kunkel, K. E., K. Hubbard, K. Redmond, K. Andsager, M. Kruk, and M. Spinar (2005), Quality control of pre-1948 cooperative observernetworkdata, *J. Atmos. Oceanic Technol.*, *22*, 1691–1705.

Kunkel, K. E., T. R. Karl, and D. R. Easterling (2007), A Monte Carlo assessment of uncertainties in heavy precipitation frequency variations, *J. Hydrometeorol.*, *8*, 1152–1160, doi:10.1175/JHM632.1.

Kunkel, K. E., D. R. Easterling, D. R. Kristovich, B. Gleason, L. Stoecker, and R. Smith (2012a), Meteorological causes of the secular variations in observed extreme precipitation events for the conterminous United States, *J. Hydrometeorol.*, *13*, 1131–1141, doi:10.1175/JHM-D-11-0108.1.

Kunkel, K. E., et al. (2012b), Monitoring and understanding trends in extreme storms: State of knowledge, *Bull. Am. Meteorol. Soc.*, *94*, 499–514, doi:10.1175/BAMS-D-11-00262.1.

Lehmann, J., D. Coumou, and K. Frieler (2015), Increased record-breaking precipitation events under global warming, *Clim. Change*, doi:10.1007/s10584-015-1434-y.

Min, S. K., X. Zhang, F. W. Zwlers, and G. C. Hegerl (2011), Human contribution to more intense precipitation extremes, *Nature*, *470*, 378–381, doi:10.1038/nature09763.

Moss, R. H., et al. (2010), The next generation of scenarios for climate change research and assessment, *Nature*, *463*, 747–756, doi:10.1038/nature08823.

Pall, P., M. R. Allen, and D. A. Stone (2007), Testing the Clausius-Clapeyron constraint on changes in extreme precipitation under CO_2 warming, *Clim. Dyn.*, *28*, 351–363.
Santer, B. D., et al. (2007), Identification of human-induced changes in atmospheric moisture content, *Proc. Natl. Acad. Sci. U. S. A.*, *104*, 15,248–15,253.
Sheffield, J., et al. (2013), North American climate in CMIP5 experiments. Part I: Evaluation of historical simulations of continental and regional climatology, *J. Clim.*, *26*, 9209–9245, doi:10.1175/JCLI-D-12-00592.1.
Sriver, R. L., C. E. Forest, and K. Keller (2015), Effects of initial conditions uncertainty on regional climate variability: An analysis using a low-resolution CESM ensemble, *Geophys. Res. Lett.*, *42*, 5468–5476, doi:10.1002/2015GL064546.
Taylor, K. E., R. J. Stouffer, and G. A. Meehl (2009), A summary of the CMIP5 experiment design, *PCDMI Rep.*, 33 pp. [Available online at http://cmip-pcmdi.llnl.gov/cmip5/docs/Taylor_CMIP5_design.pdf.]
Taylor, K. E., R. J. Stouffer, and G. A. Meehl (2012), An overview of CMIP5 and the experiment design, *Bull. Am. Meteorol. Soc.*, *93*, 485–498, doi:10.1175/BAMS-D-11-00094.1.
Trenberth, K. E., A. Dai, R. M. Rasmussen, and D. B. Parsons (2003), The changing character of precipitation, *Bull. Am. Meteorol. Soc.*, *84*, 1205–1217.
Van Vuuren, D. P., et al. (2011), The representative concentration pathways: An overview, *Clim. Change*, *109*, 5–31, doi:10.1007/s10584-011-0148-z.
Wehner, M. F. (2012), Very extreme seasonal precipitation in the NARCCAP ensemble: Model performance and projections, *Clim. Dyn.*, *40*, 59–80, doi:10.1007/s00382-012-1393-1.
Wentz, F. J., and M. Schabel (2000), Precise climate monitoring using complementary satellite data sets, *Nature*, *403*, 414–416.
Willett, K. M., N. P. Gillett, P. D. Jones, and P. W. Thorne (2007), Attribution of observed surface humidity changes to human influence, *Nature*, *449*, 710–712.
Wuebbles, D., et al. (2013), CMIP5 Climate Model Analysis. Climate Extremes in the United States, *Bull. Am. Meteorol. Soc.*, 571–583, doi:10.1175/BAMS-D-12-00172.1.